

Effect of Water Evaporation on the Inhibition of Spontaneous Coal Combustion

Qing Han, Chuanbo Cui,* Shuguang Jiang, Cunbao Deng, and Zhixin Jin

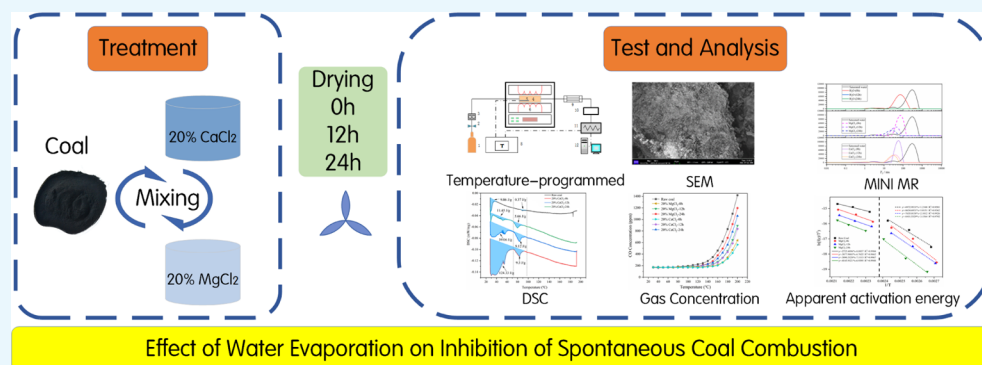
Cite This: *ACS Omega* 2022, 7, 6824–6833

Read Online

ACCESS |

Metrics & More

Article Recommendations



ABSTRACT: Spontaneous coal combustion is the primary cause of coal mine fires. During the production process, spontaneous coal combustion in the goaf is often affected by air leakage, which weakens or annuls the effect of inhibitors and leads to secondary oxidation. However, the action mechanism of inhibitors on secondary oxidation spontaneous coal combustion remains unclear. Thus, this study analyzes the influence of moisture evaporation on the performance of a high-water-content physical inhibitor (HWPI) using the Carbolite temperature-programmed experiment, differential scanning calorimetry, scanning electron microscopy, and a MINI MR test. The results demonstrate that as the moisture content of the inhibitor decreased, after being treated with the HWPI and drying for 24 h, the concentrations of O₂, CO, and CO₂ were found to be lower than the gas concentration of raw coal, which showed that although the moisture content is reduced, the treated coal sample still has a lower spontaneous combustion tendency than the raw coal. The apparent activation energy was reduced, and the heat absorption per unit time decreased, which eventually weakened or annulled the effect of the HWPI. Future research should further improve existing inhibitor types to reduce the impact of secondary oxidation on spontaneous coal combustion caused by water evaporation.

1. INTRODUCTION

In recent years, the proportion of coal in primary energy consumption in China has continually increased.^{1–3} However, coal mine environments are closed spaces prone to widespread spontaneous combustion, especially in the goaf. The number of fire accidents caused by the spontaneous combustion of residual coal has also increased, causing serious economic loss and threatening the personal safety of workers. Therefore, taking effective measures to prevent spontaneous coal combustion in coal mines is urgent.⁴

Spontaneous coal combustion is a complex physical and chemical reaction process that involves interaction between momentum and chemical structures.^{5–7} The low-temperature oxidation of coal is the primary cause of spontaneous coal combustion. Scholars worldwide have conducted studies on spontaneous coal combustion prevention technologies, including inert gas injections, inhibitors, and fire extinguishing gels.^{8–12} Inhibitors are physical or chemical based on their action mechanism. Currently, CaCl₂ and MgCl₂ are widely used

as physical inhibitors and usually mixed with water to prepare a high-water-content inhibitor solution.¹³ Physical inhibitors can prevent spontaneous coal combustion by forming a liquid film on the coal surface to isolate from oxygen contact; reduce the pore structure, size, and specific surface area; slow the water evaporation rate; and cool the coal surface.^{14–16} Moisture plays an important role in the process of inhibiting spontaneous coal combustion by effectively reducing the surface temperature of the coal and preventing the reaction of coal and oxygen.

The effect of moisture on spontaneous coal combustion is complex and has attracted the attention of many scholars.

Received: November 15, 2021

Accepted: February 4, 2022

Published: February 17, 2022



Higher moisture content generally has a significant inhibition effect. Kadioğlu and Varamaz used the crossing point method and found that the risk of spontaneous combustion increased as the air-drying time increased.¹⁷ Zhong et al. measured the heat flux and identified a critical moisture content for water-immersed and air-dried coal that heightened the probability of spontaneous combustion.¹⁸ Xu et al. used thermogravimetric analysis–differential scanning calorimetry (DSC) to study the critical moisture content at which coals were most prone to spontaneous combustion.¹⁹ Water immersion lowers the temperature of the coal and has different effects on the coal pore structure and functional groups. Song et al. analyzed the effect of water immersion on spontaneous coal combustion by crossing point temperature (CPT), scanning electron microscopy (SEM), and nitrogen adsorption and found that the average pore size of coal soaked in water was larger; additionally, the type and concentration of free radicals were higher.²⁰ Thus, long-term water immersion of residual coal in the goaf partially dissolves organic and inorganic matter and changes the physical and chemical properties.^{21,22} Zhou, Xu, and Zhuang et al. found that the changes in functional groups during spontaneous coal combustion are primarily reflected in the hydroxyl, carboxyl, and carbonyl functional groups.^{23–25} Pan et al. found that the influence of moisture on spontaneous coal combustion is primarily reflected by changes in oxygen-containing functional groups.²⁶

Researchers have conducted abundant research on the inhibition mechanisms and the influence of water content on the characteristics of spontaneous coal combustion. However, air leakage in the goaf inhibits water evaporation and weakens or annuls the inhibitory effect, which leads to secondary oxidation of coal and increases the probability of spontaneous combustion. Moreover, the influence mechanism of water evaporation on secondary oxidation spontaneous coal combustion is unclear. Thus, this study was based on the background of goaf air leakage and used a high-water-content physical inhibitor (HWPI) of 20% CaCl₂ and 20% MgCl₂ to analyze the influence of water content on the inhibitor performance.

The water evaporation experiment, Carbolite temperature-programmed experiment, DSC, SEM, and low-field nuclear magnetic resonance (NMR) were used to evaluate the influence of water content on residual secondary oxidation spontaneous coal combustion in the goaf. The results of this study provide theoretical and practical guidance for the prevention and control of spontaneous coal combustion in the goaf.

2. RESULTS AND DISCUSSION

2.1. Influence of Evaporation on Coal Moisture and Volatility. Table 1 shows the weight change and moisture content of 5 g of raw coal and 1.8 g of HWPI after drying for 0, 12, and 24 h. After prolonged drying, the evaporation of water in

Table 1. Weight Loss and Moisture of Raw Coal with the HWPI for Different Drying Times

sample	water evaporation quantity (g)	coal moisture (%)
20% CaCl ₂ -0 h	0	21.18
20% CaCl ₂ -12 h	0.76	11.26
20% CaCl ₂ -24 h	1.04	6.94
20% MgCl ₂ -0 h	0	21.18
20% MgCl ₂ -12 h	0.7	12.13
20% MgCl ₂ -24 h	0.98	7.90

the coal samples increased. For the 20% CaCl₂ inhibitor, the water content decreased from 21.18 to 11.26 and 6.94% after drying for 12 and 24 h, respectively; for the 20% MgCl₂ inhibitor, the water content decreased from 21.18 to 12.13 and 7.9% after drying for 12 and 24 h, respectively. Thus, for the same drying conditions, the water content of the coal sample after spraying with 20% MgCl₂ was higher than that after treatment with 20% CaCl₂. After evaporation in air for 12 h, the moisture content of the coal after being treated with 20% MgCl₂ and 20% CaCl₂ decreased by 42.72 and 46.86%, respectively, and for 24 h by 62.70 and 67.23%, respectively. By comparing the difference between different inhibitors, it can be calculated that the content of moisture evaporation of coal after being treated with 20% CaCl₂ was higher than that of 20% MgCl₂ by 4.08% in 12 h and 4.53% in 24 h. Therefore, the 20% MgCl₂ inhibitor produced less moisture evaporation and enhanced the water-holding capacity. Table 2 presents the results of the

Table 2. Industrial Analysis of Coal Samples (GB/T 212-2008)

sample	M _{ad} (%)	A _{ad} (%)	V _{ad} (%)	F _{cad} (%)
raw coal	2.11	24.26	27.92	45.71
20% CaCl ₂ -0 h	20.27	13.59	26.46	39.68
20% CaCl ₂ -12 h	11.31	18.70	28.60	41.39
20% CaCl ₂ -24 h	4.67	22.11	29.72	43.50
20% MgCl ₂ -0 h	20.03	13.25	26.51	40.21
20% MgCl ₂ -12 h	12.63	17.05	28.16	42.16
20% MgCl ₂ -24 h	5.78	22.8	28.86	42.56

industrial analysis of the samples for moisture, volatile matter, ash, and fixed carbon. The results in Tables 1 and 2 reveal the small differences between the industrial analysis and the weighing method. Comparing the treatment conditions reveals that the content of volatile matter, ash, and fixed carbon was higher for the lower water content, indicating that the possibility of spontaneous coal combustion increased as the drying time increased. Therefore, the inhibitor should be regularly sprayed on the coal in the goaf to reduce the risk of spontaneous combustion.

2.2. Influence of Moisture on the Low-Temperature Oxidation Index Gas. The low-temperature oxidation of coal primarily depends on the oxidation kinetic theory of the reaction between coal and oxygen.^{27–29} The theory proposes that specific active groups on the coal surface undergo an exothermic reaction upon contact with oxygen. The heat that is released promotes other reactions with higher activation energy. Therefore, inhibiting the oxidation of active groups on the coal surface is the key to inhibiting low-temperature coal oxidation. During the temperature-programming process, changes in the concentrations of CO and O₂ index gases produced from coal are used to measure the degree of coal oxidation. Thus, this study primarily focused on the concentration changes of CO and O₂ to evaluate the effect of the HWPI. Figures 1 and 2 show the CO and O₂ concentrations of raw coal with the HWPI for different drying times.

Dried samples were subjected to a temperature-programming experiment, during which part of the O₂ in air in contact with the coal sample was consumed, generating CO. The concentrations of CO, O₂, and CO₂ were measured as the gas flowed through each sensor. According to the existing research results, CO and CO₂ were the two important gases generated in the whole process of coal oxidation and were believed to be directly related

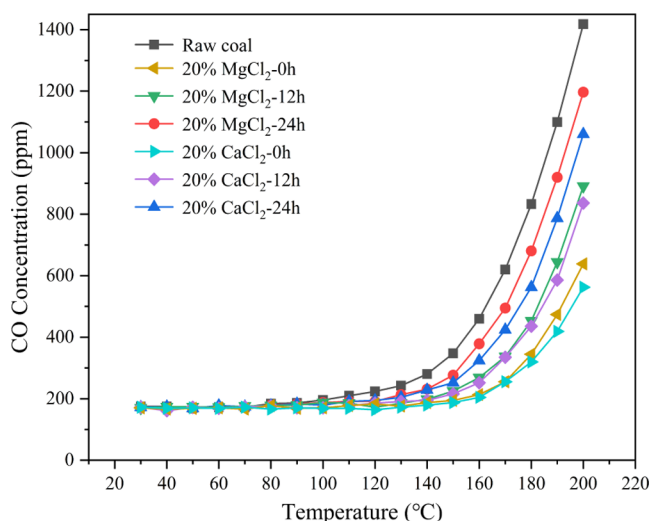


Figure 1. CO concentration of raw coal with HWPIs for different drying times.

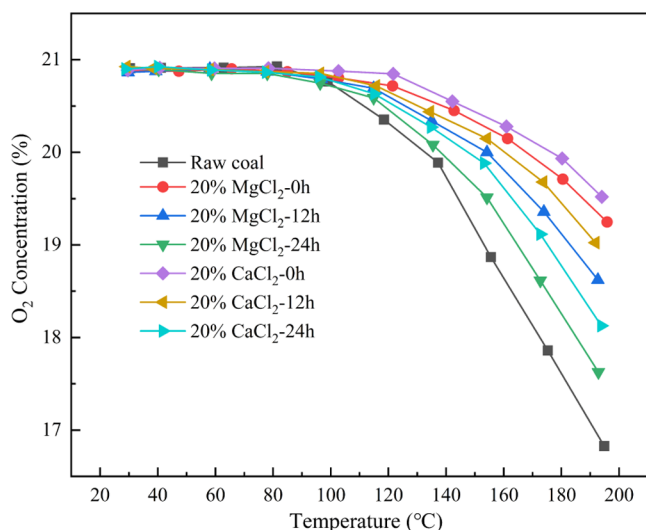


Figure 2. O₂ concentration of raw coal with HWPIs for different drying times.

to the coal spontaneous combustion mechanism.³² The larger the concentration of the two gases produced, the higher the spontaneous combustion tendency of the coal.

The CO production rate trend was divided into two sections (Figure 1). From 40 to 80 °C, the samples produced similar amounts of CO, and the production rate of specific samples gradually increased after 80 °C. The dried coal samples treated with the HWPI had lower CO production rates than the raw coal samples at the same temperature, and CO concentrations increased as the drying time of the coal samples with the HWPI increased. The moisture content of the coal sample treated with the HWPI decreased with drying, significantly inhibiting the effect of the HWPI.

Figure 2 shows the O₂ concentrations of raw coal with HWPIs for different drying times. The oxygen consumption rate of all the samples is nearly constant from 40 to 80 °C and increases significantly from 80 to 200 °C. At the same temperature, longer drying times correspond to higher oxygen consumption rates and lower moisture content, which weaken the oxygen isolation of water-wrapped coal and the inhibitory effect of the HWPI.

As shown in Figure 3, the variation law of CO₂ concentration is consistent with that of CO concentration. In coal oxidation,

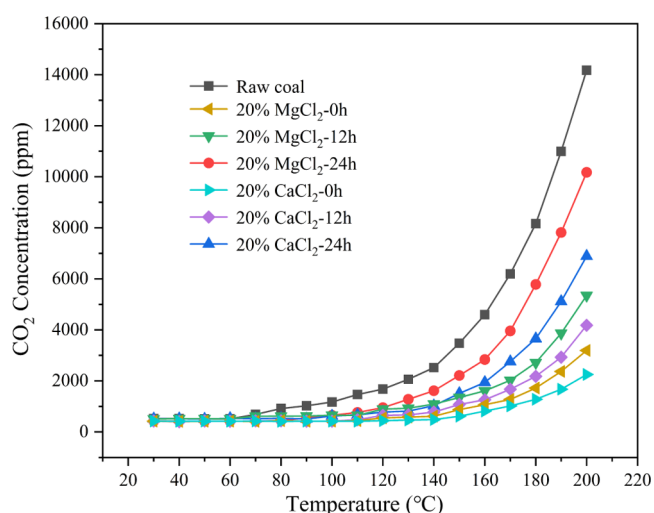


Figure 3. CO₂ concentration of raw coal with HWPIs for different drying times.

the corresponding CO₂ production also shows a rising trend with the increase of temperature. However, compared with the change of CO concentration, the concentration of CO₂ is higher, and higher CO₂ concentration corresponds to higher CO concentration, which indicates that coal is more prone to spontaneous combustion under the corresponding conditions. The CO₂ production of raw coal samples without HWPI treatment was the highest at each temperature point. At the same time, the CO₂ production of samples after HWPI treatment increased with the extension of drying time, but the corresponding CO production was lower than that of raw coal. The results show that HWPI treatment can effectively slow down the oxidation rate of the coal matrix, resulting in decreased coal spontaneous combustion tendency. With the extension of drying time, the composition effect of the inhibitor decreases gradually.

2.3. Influence of Water Evaporation on Apparent Activation Energy during the Low-Temperature Oxidation of Coal after HWPI Treatment. Low-temperature oxidation of coal is a complex process involving oxygen adsorption and the release of other gas products. Solid products also adhere to the coal surface. During the reaction of coal and oxygen on the coal surface, the changes in the internal surface area can be ignored and the oxygen consumption rate can be regarded as the rate of the entire chemical reaction. The relationship between the oxygen consumption rate v and the oxygen concentration c can be expressed as $v = -dc/dt = kc^n$, where n is the reaction order and t (s) is the reaction time. Combining the calculation method of the reaction rate and the Arrhenius formula further derives the reaction consumption rate in Formula 1

$$-\frac{dc}{dt} = A e^{-E_a/RT} c^n \quad (1)$$

where c is the oxygen concentration (mol/m³); E_a is the apparent activation energy (J/mol); A is the prefactor; and R is the gas constant, 8.314 J/(mol·K).

To simplify the calculation, we define the heating rate of the program as $w = dT/dt$ and assume that the ambient heat can be

quickly transferred to the coal. Thus, Formula 1 can be converted into Formula 2

$$-\frac{d c}{d T} = \frac{A}{w} e^{-E_a/RT} c^n \quad (2)$$

After a series of conversions and fittings, the apparent activation energy of the coal samples can be expressed by eq 3

$$\ln(f(c)/T^2) = \ln(AR/wE_a) - \frac{E_a}{RT} \quad (3)$$

Based on the Arrhenius formula and Formula 3, the apparent activation energies of the coal samples treated with 20% CaCl₂ and 20% MgCl₂ are shown in Figures 4 and 5; the fitting degree

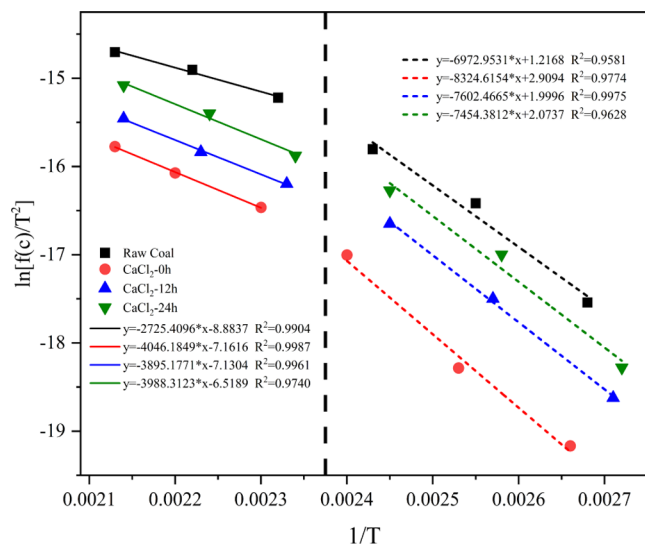


Figure 4. Apparent activation energy of samples with 20% CaCl₂.

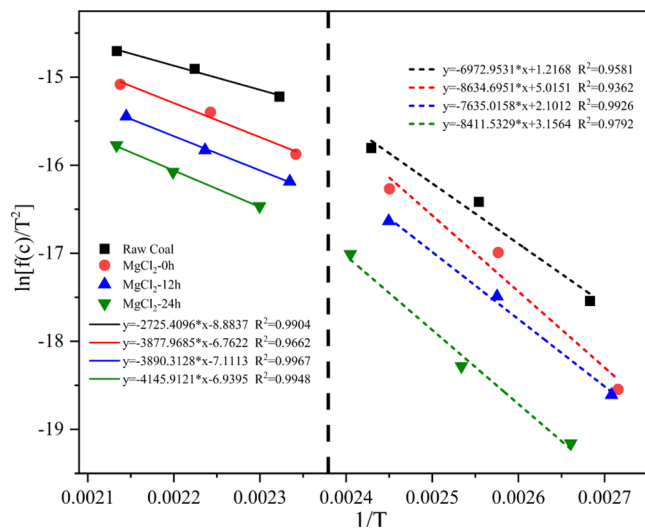


Figure 5. Apparent activation energy of samples with 20% MgCl₂.

R^2 exceeded 0.90. Based on eq 3, the intercept of $\ln(AR/wE_a)$ and the slope of $-E_a/R$ can be used to calculate the apparent activation energy E_a , where R is the gas constant [8.314 J/(mol·K)]. The results are shown in Table 3.

By analyzing the change trend of CO and O₂ gas concentration in Figure 1 and Figure 2, it can be seen that when the temperature is lower than 100 °C, the change of gas

concentration is not obvious. The main reason is that the gas in the experiment is dry air, and the influence of moisture content on spontaneous coal combustion is mainly reflected in the dehydration and accelerated oxidation stages (temperature higher than 100 °C). Therefore, this study mainly analyzed the change of activation energy in the range of 100–200 °C. Among them, by comparing the slope changes of fitting curves in different time ranges, the curves in this region can be divided into two parts, 100–140 and 140–200 °C, respectively. By comparing and analyzing the change law of activation energy in the two ranges, the change of the resistance ability of the inhibitor in the process of temperature rise can be further clarified.

In the range of 100–140 °C, the apparent activation energy of raw coal is 57.9731 kJ/mol, which is lower than that of the coal samples treated with the HWPI, indicating that the energy consumption of raw coal in the same temperature range is lower than that of the other samples; thus, the raw coal is more easily oxidized. When the temperature is in the range of 140–200 °C, the apparent activation energy of raw coal is 22.6591 kJ/mol, which is significantly lower than that of the coal samples treated with the HWPI. It can also be found that the apparent activation energy of coal in the range of 140–200 °C was lower than that in the range of 100–140 °C, from which it can be easily found that spontaneous combustion of coal is more likely to occur at a higher temperature. Comparing the apparent activation energy of the coal after treatment with the same inhibitor for different drying times revealed that the apparent activation energy during the temperature-programming process decreased as the drying time increased. This phenomenon was primarily caused by the lower moisture content of the coal after long drying times; during the temperature-programming process, coal is more easily exposed to oxygen, lowering the activation energy required for oxidation. When the moisture content of coal is low, the amount of water evaporated per unit time decreases. The amount of heat absorbed simultaneously decreases, resulting in an apparent increase in the activation energy of the low-moisture coal treated with the HWPI. In the range of 100–140 °C, the apparent activation energies of the coal samples treated with 20% CaCl₂ for 0, 12, and 24 h were 69.2019, 63.2069, and 61.9757 kJ/mol, respectively. Also, in the range of 100–140 °C, the apparent activation energies of the coal samples treated with 20% CaCl₂ for 0, 12, and 24 h were 33.6400, 32.3845, and 33.1588 kJ/mol, respectively. Compared with the apparent activation energies of the raw coal, it was only 57.9731 and 22.6591 kJ/mol. After being treated with 20% CaCl₂ and drying for 24 h, the apparent activation energy was found to be higher than that of the raw coal dried for 24 h by 10.4997 kJ/mol. Thus, it was apparent that the inhibition effect of the HWPI was significant.

Similarly, the apparent activation energy of the coal treated with 20% MgCl₂ was lower for longer drying times. After drying for 24 h, the apparent activation energy decreased to 69.9337 and 34.4691 kJ/mol and 11.9606 and 11.8101 kJ/mol, higher than that of the raw coal, respectively. These results further explained that the inhibition effect of the HWPI on spontaneous coal combustion is weakened after the moisture content of the treated coal is reduced.

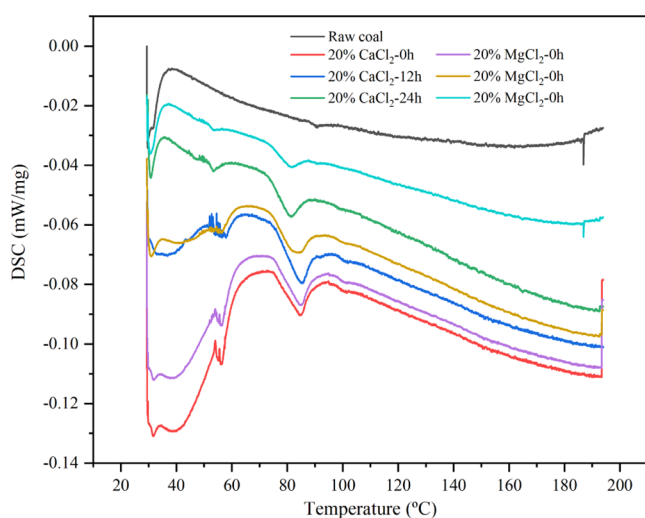
2.4. Heat Absorption and Desorption Rate of Coal Samples with Different Moisture Contents. The analysis results of the moisture content and surface activation energy of coal samples treated with the HWPI for different drying times revealed that one of the reasons for the high activation energy of

Table 3. Apparent Activation Energy E_a : 100–200 °C (kJ/mol)

sample	slope ^a	slope ^b	intercept ^a	intercept ^b	E_a^a	E_a^b	R^{2a}	R^{2b}
raw coal	−6972.9531	−2725.4096	1.2168	−8.8837	57.9731	22.6591	0.9581	0.9904
20% CaCl ₂ -0 h	−8324.6154	−4046.1849	2.9094	−7.1616	69.2109	33.6400	0.9774	0.9987
20% CaCl ₂ -12 h	−7602.4665	−3895.1774	19.996	−7.1304	63.2069	32.3845	0.9975	0.9961
20% CaCl ₂ -24 h	−7454.3812	−3988.3123	2.0737	−6.5189	61.9757	33.1588	0.9628	0.9740
20% MgCl ₂ -0 h	−8634.6951	−3877.9865	5.0151	−6.7622	71.7889	32.2416	0.9362	0.9662
20% MgCl ₂ -12 h	−7635.0158	−3890.3128	2.1012	−7.1113	63.4775	32.3441	0.9926	0.9967
20% MgCl ₂ -24 h	−8411.5629	−4145.9121	3.1564	−6.9395	69.9337	34.4691	0.9792	0.9948

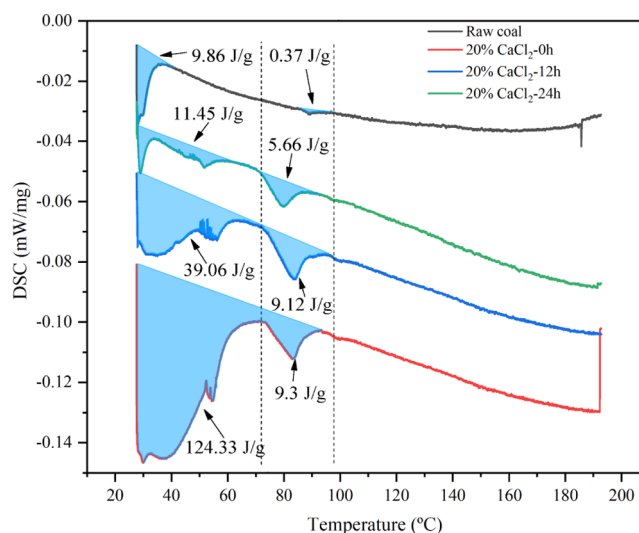
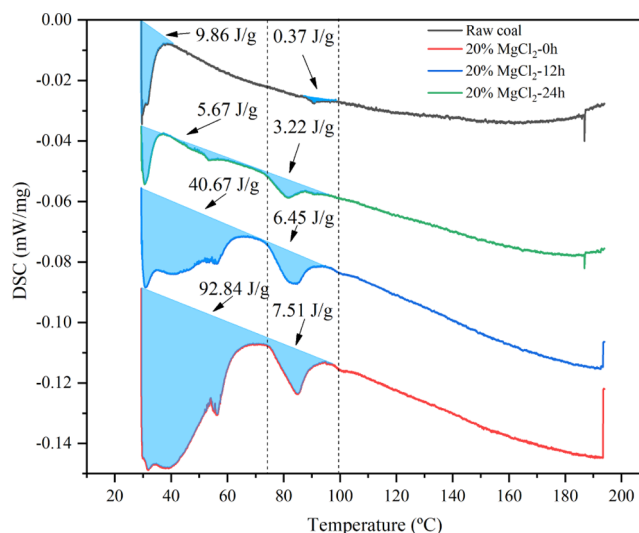
^a1/T > 0.0024. ^b1/T < 0.0024.

low moisture content coal is the lower water evaporation per unit time, which lowers heat absorption and requires more heat of oxidation for chemical reactions. Section 2.3 presented the apparent activation energy of the coal samples. To accurately analyze the heat absorption of water evaporation in the temperature-programming process, a differential scanning calorimeter produced by TA in the United States was used to analyze the heat absorption and desorption rate of coal samples with different moisture contents. The abundant heat released in the reaction between coal and oxygen affects the determination of heat absorption; thus, 80 mL/min N₂ was injected during the reaction. Figure 6 shows the DSC test results for the samples, and Figure 8 shows the changes in the endothermic peak for different drying times.

**Figure 6.** DSC results of different samples.

Well-defined endothermic peaks appear in the 30–74 and 74–98 °C ranges for different samples (Figures 7 and 8). The results show that the moisture in the coal completely evaporates before the temperature reaches 100 °C. The endothermic capacity from 30 to 74 °C is much greater than that from 74 to 98 °C, indicating that much moisture is completely evaporated at temperatures less than 74 °C.

Compared to the difference between the DSC curves of the coal samples, the endothermic peaks of raw coal were relatively weak. From 74 to 98 °C, the endothermic peak almost disappeared. For the coal samples treated with the same inhibitor, the peak value and area from 30 to 74 °C gradually decreased as the drying time increased, possibly because the evaporation of moisture reduces the heat absorption of the sample per unit time. However, from 74 to 98 °C, the heat

**Figure 7.** DSC results of samples with 20% CaCl₂.**Figure 8.** DSC results of samples with 20% MgCl₂.

absorption values of the coal samples treated with various inhibitors were similar.

To further analyze and express the heat absorption capacity during water evaporation in the two temperature ranges, the corresponding peak area was calculated. Figure 9 shows the changes in the heat absorption under different treatment conditions. The heat adsorption capacities of raw coal from 30 to 74 °C (9.86 J/g) and from 74 to 98 °C (0.37 J/g) were lower than those of other samples. The heat adsorption capacities of the coal sample treated with 20% CaCl₂ for 0, 12, and 24 h were

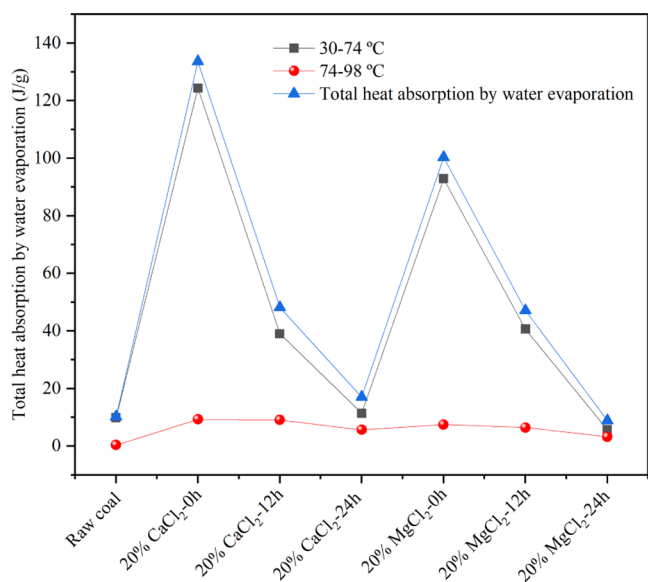


Figure 9. Heat absorption by the evaporation of different samples.

124.33, 39.06, and 11.45 J/g at 30–74 °C and 9.31, 9.12, and 5.66 J/g at 74–98 °C, respectively. The heat adsorption capacity of the coal sample treated with 20% MgCl₂ and dried for 0, 12, and 24 h were 92.84, 40.67, and 5.67 J/g at 30–74 °C and 7.51, 6.45, and 3.22 J/g at 74–98 °C, respectively. Therefore, the heat absorption capacity decreases as the moisture content is reduced, and the amount of water evaporated is lower at higher temperatures. Additionally, we compared the results of different treatment conditions and found that 20% MgCl₂ had a better inhibition effect.

2.5. SEM Results and Analysis. In this paper, we use SEM as an auxiliary means to analyze the morphology and structure of the coal surface corresponding to different drying times after HWPI treatment. Overall, after HWPI treatment, the roughness of the coal surface is significantly reduced. Figure 10b–d shows the results of drying for 12 h after H₂O and HWPI treatments, respectively. It is obvious that the coal surface after HWPI treatment is more wrapped and the coal surface after 20% MgCl₂ treatment is denser and smoother than that after 20% CaCl₂ treatment. It can be deduced that the inhibition effect of 20% MgCl₂ spraying is more obvious.

Figure 10e–g shows the results of drying for 24 h after H₂O and HWPI treatments, respectively. With the extension of drying time, pores and cracks appear on the surface structure of coal under different treatment conditions to a certain extent. Among them, pores and cracks can be obviously observed in the red area in Figure 10f,g. The results showed that with the extension of drying time, the inhibition effect of the inhibitor is gradually weakened, but compared with the coal sample without inhibitor treatment (Figure 10e), the coal surface was still relatively flat and obviously wrapped. The results showed that the HWPI had a better inhibition effect than H₂O. At the same time, by comparing the surface structure characteristics of coal after drying for 12 and 24 h after 20% CaCl₂ and 20% MgCl₂ treatment, it can be seen that the surface structure of coal after drying for 24 h after 20% CaCl₂ treatment shows pores and cracks compared with that after drying for 12 h, but the surface structure of coal after 20% MgCl₂ treatment has no significant change compared with that after drying for 12 h. In other words, the inhibition effect of 20% MgCl₂ is more ideal and is less affected by the drying time compared with that of 20% CaCl₂.

2.6. MINI MR Results and Analysis. Figure 11 shows the MINI MR test results of the coal samples treated with different inhibitors for different treatment times. The results show that

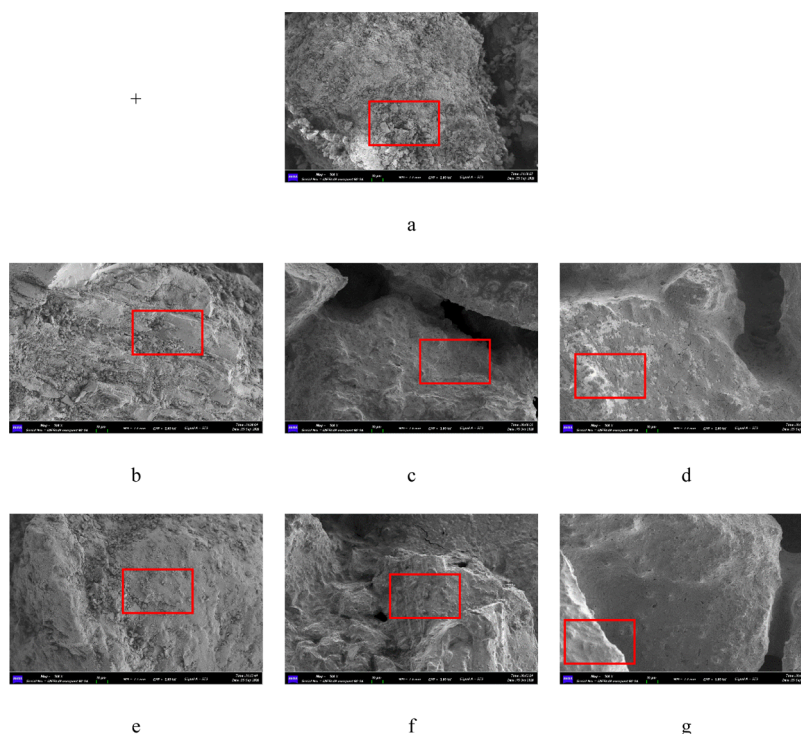


Figure 10. SEM results of coal samples before and after treatment with H₂O and HWPI. (a) Raw coal (untreated); (b) H₂O-12 h; (c) CaCl₂-12 h; (d) MgCl₂-12 h; (e) H₂O-24 h; (f) CaCl₂-24 h; and (g) MgCl₂-24 h.

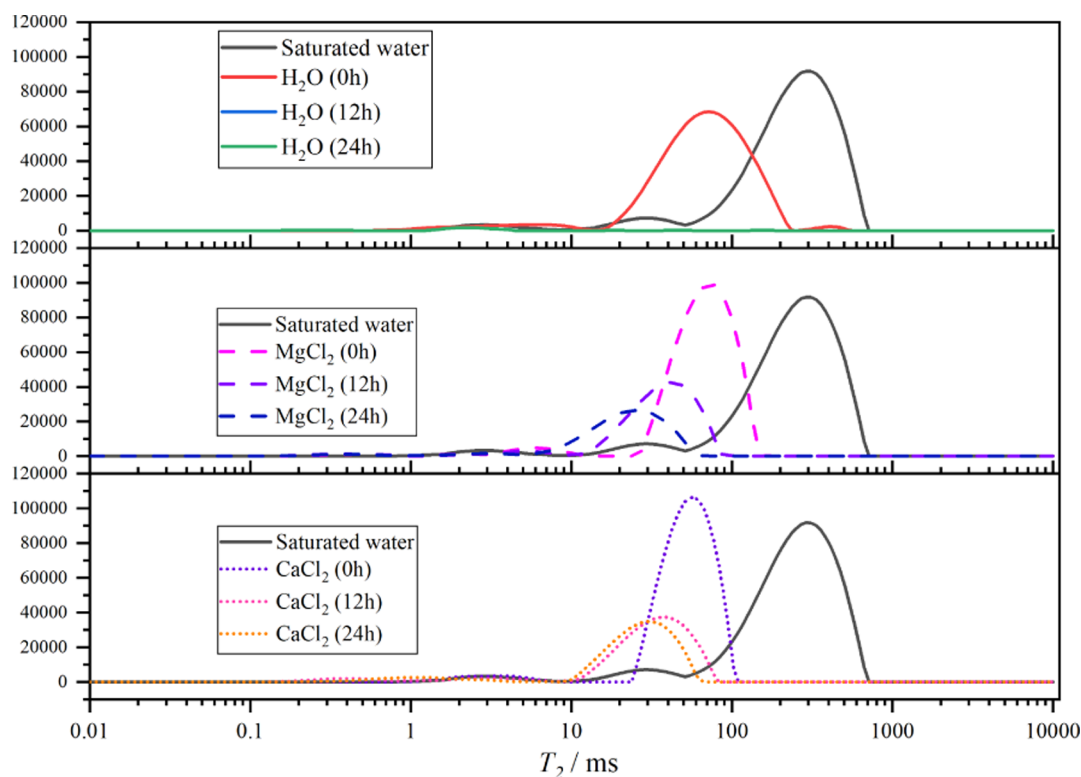


Figure 11. T_2 spectra for coal samples.

the relaxation time T_2 is positively correlated with the change in the pore size. The T_2 spectrum in Figure 11 ranges from 0.01 to 10 000 ms, which corresponds to coal macropores, mesopores, and micropores. The measured results generally corresponded to micropores, mesopores, and macropores for relaxation times of <10, 10–100, and >100 ms, respectively.

Figure 11 shows the large differences in the T_2 spectrum between the water-saturated coal and centrifuged coal samples, indicating that the proportion of closed pores in coal increased as the water content decreased. The pore structures of the coal samples treated with H_2O and HWPI changed from macropores to mesopores. The pore structure of the coal samples after treatment with the HWPI was primarily composed of mesopores, and the peak width was smaller than that of the coal samples treated with H_2O . As the drying time increased, the mesopore peak range of 10–100 ms moved to the left after treatment with $MgCl_2$ and $CaCl_2$ and drying for 12 and 24 h, and the peak height gradually decreased. Therefore, the pore structure distribution of coal gradually transitions from mesopores to micropores as the water evaporation time increases. Micropores are not conducive to methane diffusion in coal.^{30,31} Thus, after treatment with the HWPI, the pore structure of coal changes, and the dense pore structure significantly reduces the risk of spontaneous coal combustion. However, the amount of water in the HWPI decreases as the drying time increases, weakening or annulling the function of the original liquid membrane isolation, gradually exposing the surface of the pore structures, and increasing the risk of spontaneous combustion.³³ Therefore, although inhibitors can partially change the coal structure, a decrease in moisture weakens the blocking effect and increases the risk of spontaneous coal combustion.

3. CONCLUSIONS

The strong fluidity and easy evaporation properties of the HWPI reduce its inhibitory effect after spraying in the goaf. Thus, studying the influence of the water evaporation rate of inhibitors on spontaneous coal combustion caused by air leakage in the goaf is important. The following conclusions are drawn from this study:

- (1) After treatment with the HWPI, the moisture content of the coal samples gradually decreased as the drying time increased; additionally, the ability of water to isolate the coal from oxygen and the inhibition effect were gradually weakened. At the same temperature, oxygen consumption rates are higher for longer drying times. The CO concentration of the samples with added HWPI was lower than that of the untreated raw coal samples, indicating that the HWPI reduces the influence of water evaporation on spontaneous coal combustion.
- (2) Low-temperature oxidation of coal is a complex process involving oxygen adsorption and gas product release. Analyzing the apparent activation energy of coal samples reveals that raw coal is more easily oxidized than the coal samples treated with the HWPI. As the drying time increased, the endothermic capacity and apparent activation energy required for the oxidation of the coal samples treated with the inhibitor continuously decreased; therefore, the inhibition effect of spontaneous coal combustion weakened or disappeared as the moisture content of the coal samples treated with the HWPI decreased.
- (3) After spraying the HWPI into the goaf, the small particles on the coal surface were consolidated, reducing the contact between the coal and air. Additionally, the pore structure of the coal after treatment with the HWPI

Table 4. Proximate and Elemental Coal Sample Analyses³⁴

proximate analysis (%)				ultimate analysis (%)				
M_{ad}	A_d	V_{daf}	F_{Cad}	C_{daf}	H_{daf}	O_{daf}	N_{daf}	S_{daf}
2.38	25.32	40.96	43.04	78.49	5.10	13.42	1.45	1.15

gradually changed from macropores to mesopores, effectively reducing the risk of spontaneous combustion. However, as the moisture evaporation increased, the coal surface showed significant pore and fracture structures that weakened the wrapping effect of the inhibitor. As the area of the coal surface was increasingly exposed to air, the risk of spontaneous combustion increased; thus, the inhibition effect of the HWPI was reduced or annulled.

4. MATERIALS AND METHODS

4.1. Coal Sample Collection and Preparation. The fresh coal samples were taken from Longdong Mine, Xuzhou City, China, and sealed in bags for transportation to the laboratory. The coal samples were ground and sieved to a 0.18–0.38 mm particle size and dried in a vacuum oven for 24 h at 40 °C. Table 4 presents the results of the proximate and ultimate analyses.³⁴

4.2. Experiment System. The testing system simulating coal acceleration combustion is a temperature-programmed analysis system composed of a PC, a data collector, an indicator gas analysis system, a thermocouple, and an electronic balance. The data acquisition system includes a Siemens CPU-224 CN, EM231 module. The indicator gas analysis system includes a high-precision CO sensor, a CO₂ sensor, an O₂ sensor, and a signal processing module. The indicator gas analysis system collects the indicator gas concentration in real time more efficiently and conveniently than a gas chromatograph. Figure 12 illustrates the experimental setup which was same as our previous study.³⁴

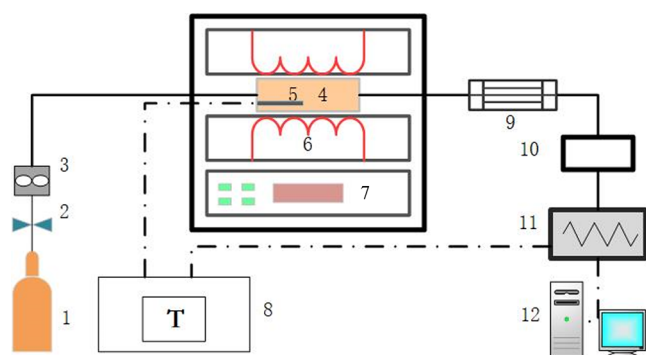


Figure 12. Testing system simulating coal acceleration combustion. 1 Dry air bottle, 2 pressure reducing valve, 3 flow sensor, 4 coal reaction vessel, 5 thermocouple, 6 heater, 7 control panel, 8 temperature display, 9 condenser, 10 indicator gas analysis system, 11 data collector, and 12 PC.³⁴

4.3. Experiment Procedures. **4.3.1. Effect of Water Evaporation on the Inhibitory Effect of the HWPI.** The following experiment was performed to study the effect of water evaporation on the inhibitory effect of HWPI. Also, the sample processing is similar to our previous papers.³⁴

Step 1: CaCl₂ and MgCl₂ were dissolved in ultrapure water to prepare CaCl₂ and MgCl₂ solutions with a final concentration of 20%.

Step 2: 30 g of dried coal samples with sizes of 0.18–0.38 mm were divided into six pieces. Three pieces were added to 1.8 g of the HWPI and stirred effectively.

Step 3: The six samples were dried in a vacuum oven at 40 °C for 12 and 24 h, respectively; and the content weights were determined. The samples under different treatment conditions were marked as 20% CaCl₂-0 h, 20% CaCl₂-12 h, 20% CaCl₂-24 h, 20% MgCl₂-0 h, 20% MgCl₂-12 h, and 20% MgCl₂-24 h.

Step 4: The six dried samples were used for industrial analysis to calculate the moisture, volatiles, and moisture reduction of coal.

4.3.2. Carbolite Temperature-Programmed Experiment. After being treated with the HWPI and the raw coal, the six coal samples were taken (3 g) and mixed with 5 g of dried raw coal, respectively. The seven coal samples including the raw coal sample were dried in a vacuum drying oven at 40 °C constant temperature for 0, 12, and 24 h, respectively. Then, the seven samples were put into the reaction vessel for performing the temperature-programmed experiment, respectively. An experiment was performed using the system shown in Figure 11 to detect the indicator gas concentration in the temperature-programming process. The experimental conditions were the following: heating range, 30–200 °C; heating rate, 2 °C/min; and dry air injection rate, 10 mL/min.³⁴

4.3.3. DSC Test for Coal Samples with Different Moisture Contents. DSC tests were conducted on the samples using the NETZSCH DSC200F3 instrument produced in Germany. After treatment under different conditions, the six coal samples were used to analyze the heat release rate. The experimental conditions were as follows: temperature range, 30–190 °C; heating rate, 1 °C/min; and N₂ injection flow rate, 80 mL/min.

4.3.4. SEM Test. The morphological changes in the coal and degraded coal were assessed using thermal field emission SEM (ZEISS, Japan). The acceleration voltage of the scanning electron microscope was 10 kV, the resolution was 1.0 mm, and the magnification was 5000–10 000 times. Before assessment, the coal samples were coated with gold using an Emitech K550 gold sputter coater.

4.3.5. MINI MR Test. The MINI MR (MesoMR12-025V, China) used in this study performs core analysis and imaging functions. The distribution and connectivity of pores and fractures were obtained by measuring the T_2 relaxation time of the fluid in the pores of the coal samples. The relaxation time T_2 is proportional to the pore size in coal. For coal, when the relaxation time T_2 is less than 10 ms, the measured pore size range represents the micropores in coal. The measured pore size range in the range of 10–100 ms is the mesopore, while the measured pore size range greater than 100 ms is the macropore. Therefore, coal samples in water saturation and other conditions were tested in this study. The T_2 spectrum of the NMR test reflects the distribution of all pores in the coal, including closed and open holes. After centrifugation, the free water in the saturated water coal sample was removed, and NMR was performed on the centrifugal coal sample. The data processing method can be found in the study of Zhang et al.²⁷

AUTHOR INFORMATION

Corresponding Author

Chuanbo Cui – College of Safety and Emergency Management and Engineering, Taiyuan University of Technology, Jinzhong 030600, China; orcid.org/0000-0002-4782-4301;
Email: hanqing0175@link.tyut.edu.cn

Authors

Qing Han – College of Safety and Emergency Management and Engineering, Taiyuan University of Technology, Jinzhong 030600, China

Shuguang Jiang – Key Laboratory of Gas and Fire Control for Coal Mines (China University of Mining & Technology), Ministry of Education, Xuzhou 221116, China; School of Safety Engineering, China University of Mining & Technology, Xuzhou 221116, China

Cunbao Deng – College of Safety and Emergency Management and Engineering, Taiyuan University of Technology, Jinzhong 030600, China

Zhixian Jin – College of Safety and Emergency Management and Engineering, Taiyuan University of Technology, Jinzhong 030600, China

Complete contact information is available at:

<https://pubs.acs.org/10.1021/acsomega.1c06418>

Notes

The authors declare no competing financial interest.

ACKNOWLEDGMENTS

This work was supported by the National Natural Science Foundation of China (U1810206 and 52074285), the Natural Science Foundation of Shanxi Province (20210302124134), and the China Postdoctoral Science Foundation (2021M690530).

REFERENCES

- (1) Gasparotto, J.; Da Boit Martinello, K. Coal as an energy source and its impacts on human health. *Energy Geosci.* **2021**, *2*, 113–120.
- (2) Guo, X.; Xiao, B.; Song, L. Emission reduction and energy-intensity enhancement: The expected and unexpected consequences of China's coal consumption constraint policy. *J. Cleaner Prod.* **2020**, *271*, 122691.
- (3) He, A.; Li, X.; Ai, Y.; Li, X.; Li, X.; Zhang, Y.; Gao, Y.; Liu, B.; Zhang, X.; Zhang, M.; Peng, L.; Zhou, M.; Yu, H. Potentially toxic metals and the risk to children's health in a coal mining city: An investigation of soil and dust levels, bioaccessibility and blood lead levels. *Environ. Int.* **2020**, *141*, 105788.
- (4) Cheng, J.; Wu, Y.; Dong, Z.; Zhang, R.; Wang, W.; Wei, G.; Chu, T.; Yu, Z.; Qin, Y.; Liu, G.; Li, H. A novel composite inorganic retarding gel for preventing coal spontaneous combustion. *Case Stud. Therm. Eng.* **2021**, *28*, 101648.
- (5) Deng, J.; Yang, Y.; Zhang, Y.-N.; Liu, B.; Shu, C.-M. Inhibiting effects of three commercial inhibitors in spontaneous coal combustion. *Energy* **2018**, *160*, 1174–1185.
- (6) Wen, H.; Wang, H.; Liu, W.; Cheng, X. Comparative study of experimental testing methods for characterization parameters of coal spontaneous combustion. *Fuel* **2020**, *275*, 117880.
- (7) Onifade, M.; Genc, B. Spontaneous combustion of coals and coal-shales. *Int. J. Min. Sci. Technol.* **2018**, *28*, 933–940.
- (8) Watanabe, W. S.; Zhang, D.-k. The effect of inherent and added inorganic matter on low-temperature oxidation reaction of coal. *Fuel Process. Technol.* **2001**, *74*, 145–160.
- (9) Si, L.; Zhang, H.; Wei, J.; Li, B.; Han, H. Modeling and experiment for effective diffusion coefficient of gas in water-saturated coal. *Fuel* **2021**, *284*, 118887.
- (10) Tang, Y. Inhibition of Low-Temperature Oxidation of Bituminous Coal Using a Novel Phase-Transition Aerosol. *Energy Fuels* **2016**, *30*, 9303–9309.
- (11) Liu, Y.; Wen, H.; Guo, J.; Jin, Y.; Wei, G.; Yang, Z. Coal spontaneous combustion and N₂ suppression in triple goafs: A numerical simulation and experimental study. *Fuel* **2020**, *271*, 117625.
- (12) Lu, Y.; Liu, Y.; Shi, S.; Wang, G. G. X.; Li, H.; Wang, T. Micro-particles stabilized aqueous foam for coal spontaneous combustion control and its flow characteristics. *Process Saf. Environ. Prot.* **2020**, *139*, 262–272.
- (13) Ma, L.; Qin, G.; Jingjing, L.; Xue, W. In Inventory management with mental accounting. *2015 12th International Conference on Service Systems and Service Management (ICSSSM)*, June 22–24, 2015; pp 1–4.
- (14) Xi, Z.; Li, D.; Feng, Z. Characteristics of polymorphic foam for inhibiting spontaneous coal combustion. *Fuel* **2017**, *206*, 334–341.
- (15) Xiao, Y.; Lü, H.-F.; Yi, X.; Deng, J.; Shu, C.-M. Treating bituminous coal with ionic liquids to inhibit coal spontaneous combustion. *J. Therm. Anal. Calorim.* **2019**, *135*, 2711–2721.
- (16) Tang, Y. Experimental investigation of applying MgCl₂ and phosphates to synergistically inhibit the spontaneous combustion of coal. *J. Energy Inst.* **2018**, *91*, 639–645.
- (17) Kadioğlu, Y.; Varamaz, M. The effect of moisture content and air-drying on spontaneous combustion characteristics of two Turkish lignites. *Fuel* **2003**, *82*, 1685–1693.
- (18) Zhong, X.; Kan, L.; Xin, H.; Qin, B.; Dou, G. Thermal effects and active group differentiation of low-rank coal during low-temperature oxidation under vacuum drying after water immersion. *Fuel* **2019**, *236*, 1204–1212.
- (19) Xu, T.; Wang, D.-M.; He, Q.-L. The Study of the Critical Moisture Content at Which Coal Has the Most High Tendency to Spontaneous Combustion. *Int. J. Coal Prep. Util.* **2013**, *33*, 117–127.
- (20) Song, S.; Qin, B.; Xin, H.; Qin, X.; Chen, K. Exploring effect of water immersion on the structure and low-temperature oxidation of coal: A case study of Shendong long flame coal, China. *Fuel* **2018**, *234*, 732–737.
- (21) Yu, J.; Tahmasebi, A.; Han, Y.; Yin, F.; Li, X. A review on water in low rank coals: The existence, interaction with coal structure and effects on coal utilization. *Fuel Process. Technol.* **2013**, *106*, 9–20.
- (22) Li, J.; Li, Z.; Yang, Y.; et al. Study on the generation of active sites during low-temperature pyrolysis of coal and its influence on coal spontaneous combustion. *Fuel* **2019**, *241*, 283–296.
- (23) Zhou, C.; Zhang, Y.; Wang, J.; Xue, S.; Wu, J.; Chang, L. Study on the relationship between microscopic functional group and coal mass changes during low-temperature oxidation of coal. *Int. J. Coal Geol.* **2017**, *171*, 212–222.
- (24) Xu, T. Heat effect of the oxygen-containing functional groups in coal during spontaneous combustion processes. *Adv. Powder Technol.* **2017**, *28*, 1841–1848.
- (25) Zhuang, L.; Ji-Ren, W. The Technology of Forecasting and Predicting the Hidden Danger of Underground Coal Spontaneous Combustion. *Procedia Eng.* **2011**, *26*, 2301–2305.
- (26) Pan, R.; Hu, D.; Chao, J.; Wang, L.; Ma, J.; Jia, H. The heat of wetting and its effect on coal spontaneous combustion. *Thermochim. Acta* **2020**, *691*, 178711.
- (27) Xu, Y.-l.; Wang, D.-m.; Wang, L.-y.; Zhong, X.-x.; Chu, T.-x. Experimental research on inhibition performances of the sand-suspended colloid for coal spontaneous combustion. *Saf. Sci.* **2012**, *50*, 822–827.
- (28) Zubiček, V.; Adamus, A. Susceptibility of coal to spontaneous combustion verified by modified adiabatic method under conditions of Ostrava–Karvina Coalfield, Czech Republic. *Fuel Process. Technol.* **2013**, *113*, 63–66.
- (29) Shi, T.; Wang, X.; Deng, J.; Wen, Z. The mechanism at the initial stage of the room-temperature oxidation of coal. *Combust. Flame* **2005**, *140*, 332–345.
- (30) Lu, G.; Wei, C.; Wang, J.; Meng, R.; Tamehe, L. S. Influence of pore structure and surface free energy on the contents of adsorbed and free methane in tectonically deformed coal. *Fuel* **2021**, *285*, 119087.

(31) Feng, G.; Niu, X.; Liao, J.; Han, Y.; Bai, Z.; Li, W. Correlation between Drying Behaviors of Brown Coal and Its Pore Structures. *Energy Fuels* **2019**, *33*, 6027–6037.

(32) Liu, Z.; Xu, Y.; Wen, X.-l.; Lv, Z.; Wu, J.; Li, M.; Wang, L. Thermal Properties and Key Groups Evolution of Low-Temperature Oxidation for Bituminous Coal under Lean-Oxygen Environment. *ACS Omega* **2021**, *6*, 15115–15125.

(33) Zhang, X.; Lin, B.; Zhu, C.; Wang, Y.; Guo, C.; Kong, J. Improvement of the electrical disintegration of coal sample with different concentrations of NaCl solution. *Fuel* **2018**, *222*, 695–704.

(34) Cui, C.; Jiang, S.; Shao, H.; et al. Experimental study on thermo-responsive inhibitors inhibiting coal spontaneous combustion. *Fuel Process. Technol.* **2018**, *175*, 113–122.